

Construction of Oroville Dam

For LUSAS version:	21.0
For software product(s):	LUSAS Bridge plus or LUSAS Civil&Structural plus
With product option(s):	Geotechnical, Nonlinear

Problem Description

The construction of the Oroville dam was modelled using the Duncan-Chang method by Kulhawy and Duncan [1]. The dam was built in three stages. At its centre is a concrete core block. A cofferdam was built in front of this and finally the main dam itself was constructed. The basic layout is shown in figure 1.

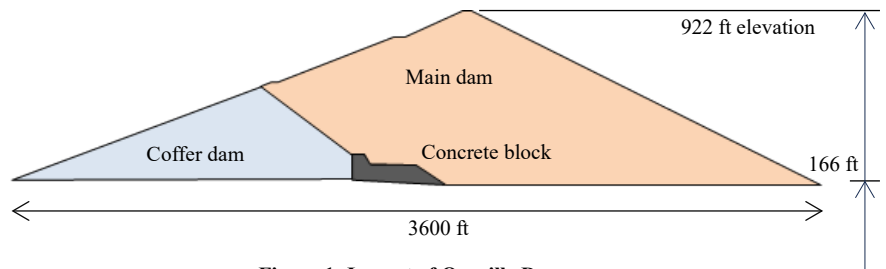


Figure 1: Layout of Oroville Dam

The modelling of the construction of the coffer dam is done by splitting it into six horizontal layers which are activated sequentially followed by the main dam using a further twelve layers. Two solutions are considered, one in which the layer is activated in a single increment, the second in which the gravity load is applied to the layer in four equal increments.

Keywords

Plane Strain, Duncan-Chang, activation, deactivation.

Associated Files

Associated files can be downloaded from the user area of the LUSAS website.



oroville_dam.lvb carries out automated modelling of the example.

- Use **File > New** to create a new model of a suitable name in a chosen location.
- Use **File > Script > Run Script** to open the lvb file named above that was downloaded and placed in a folder of your choosing.

Discretisation

The problem is modelled using quadrilateral plane strain elements, QPN8 (figure 2).

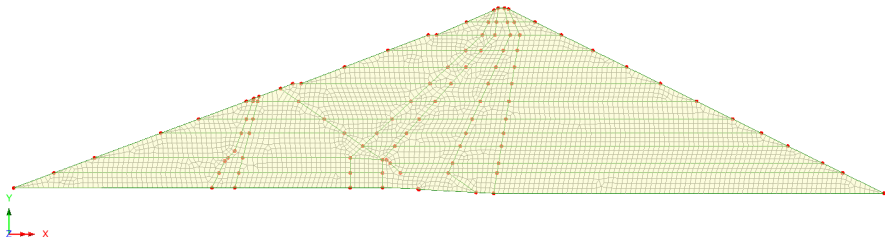


Figure 2: Model mesh

Material Properties

The dam is constructed from four materials used for the shell, the transition, the core and the concrete block as shown in figure 4.

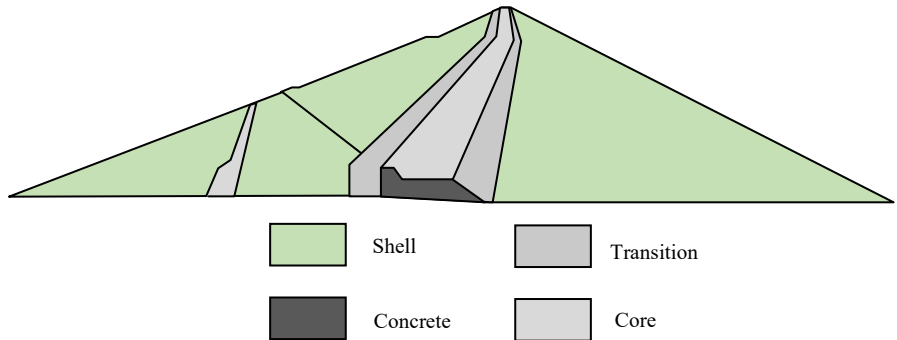


Figure 4: Layout of material layers

The soils are modelled using the Duncan–Chang material model whilst the concrete is treated as a linear elastic material. Properties are given in table 1.

Table 1: Modified Mohr-Coulomb material properties

Parameter	Shell	Transition	Core	Concrete
Young's modulus (lbf/ft ²)	-	-	-	835x10 ⁶
Density (lbs/ft ³)	150	150	150	162
Cohesion (lbf/ft ²)	0	0	2795	-
Friction angle ϕ°	43.5	43.5	25.1	-
Modulus number, K	3780	3350	345	-
Modulus number for loading/unloading, K_{ur}	4160	3685	380	-
Modulus exponent, n	0.19	0.19	0.76	-
Failure ratio, R_f	0.76	0.76	0.88	-
Atmospheric pressure, P_a (lbf/ft ²)	2116	2116	2116	-
K_0	0.312	0.312	0.576	-
Poisson's ratio / parameters	-	-	-	0.15
Poisson's ratio at atmospheric pressure, G	0.43	0.43	0.30	-
Cell pressure moderation factor, F	0.19	0.19	-0.05	-

Poisson's ratio tangent factor, D	14.8	14.8	3.83	-
Young's modulus when soil fails (lbf/ft ²)*	$\alpha.K.P_a$	$\alpha.K.P_a$	$\alpha.K.P_a$	-
Poisson's ratio on soil failure	0.49	0.49	0.49	-
Min.stress to evaluate soil stiffness (lbf/ft ²)	450	450	450	-
Max.stress in tension (lbf/ft ²)	0	0	5960	-

* The Young's modulus on failure is adjusted to give a stable solution.

Loading Conditions

Gravity is the only loading.

Theory

None. The results are compared with measured data.

Modelling Hints

Soil stiffness is related to the confining stresses holding it together. The Duncan-Chang model defines the soil stiffness using the maximum principal stress (note tension is positive). This has the disadvantage that at low stresses and when the soil goes into tension the stiffness becomes very small before dropping to zero. The LUSAS implementation includes a minimum value of pressure to define a minimum soil strength at low stress confinements. A value of one fifth of atmospheric pressure gives the strength of the soil at approximately 1m depth below the surface and is a reasonable value to use.

The Duncan-Chang method uses an incremental elastic approach to solve the stress update in which the incremental displacements are calculated from the incremental change in load and the tangential stiffness. The solution is explicit with the soil stiffness defined at the start of the increment. This provides a rapid solution to problems but one which may drift from the true solution, particularly if large increments are taken.

A key problem with the method is that the tangential stiffness goes to zero when the soil is in tension or has failed in shear. In this case, even the most minimal of loads produces infinitely large displacements. LUSAS allows the definition of a failure value of Young's modulus for soil which has lost its stiffness. In most cases, tension is very limited and in

parts of the soil that are not of engineering significance so to get a realistic solution the use of a fictitious stiffness is expedient.

In this example, the failure stiffness, E_{fail} , is defined in terms of a scale factor, α , the atmospheric pressure, P_a , and the modulus number K

$$E_{fail} = \alpha.K.P_a$$

The scale factor is increased until the first sensible solution is calculated. In figures 5 to 7 the effect of increasing the scale factor α is shown. With no failure stiffness, the solution fails at point where the soil connects to the concrete block (figure 5) during the activation of the first layer of the coffer dam.

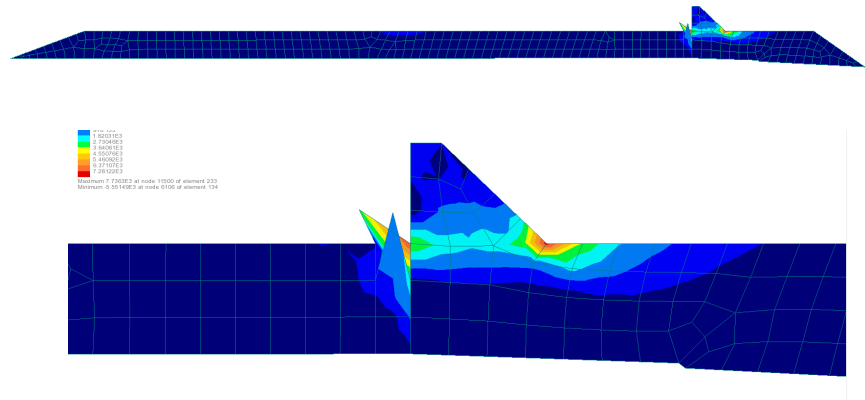


Figure 5: $\alpha=0$ - Displaced shape at failure

Applying a small stiffness with $\alpha=0.001$ advances the solution significantly with failure now occurring at connection of the soil layers in the coffer and main dam (figure 6).

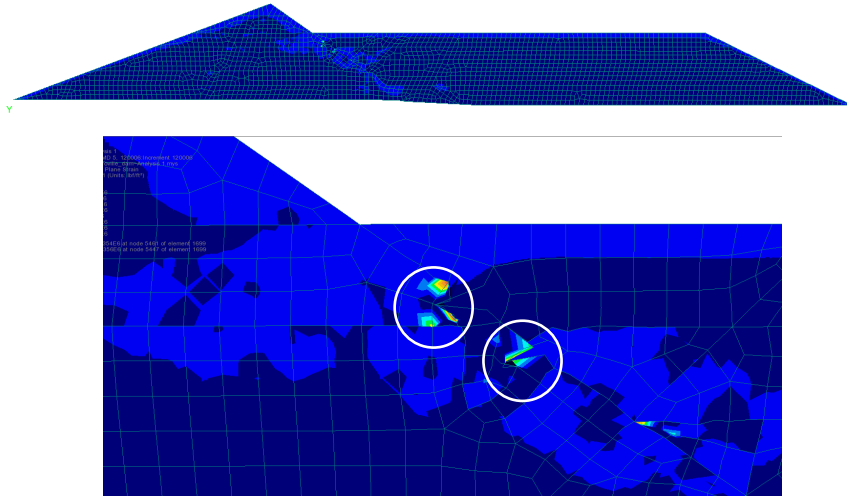


Figure 6: $\alpha=0.001$ - Displaced shape at failure

The stiffness is further increased to $\alpha=0.01$. But, again, the soil fails along the coffer dam/main dam boundary (figure 7).

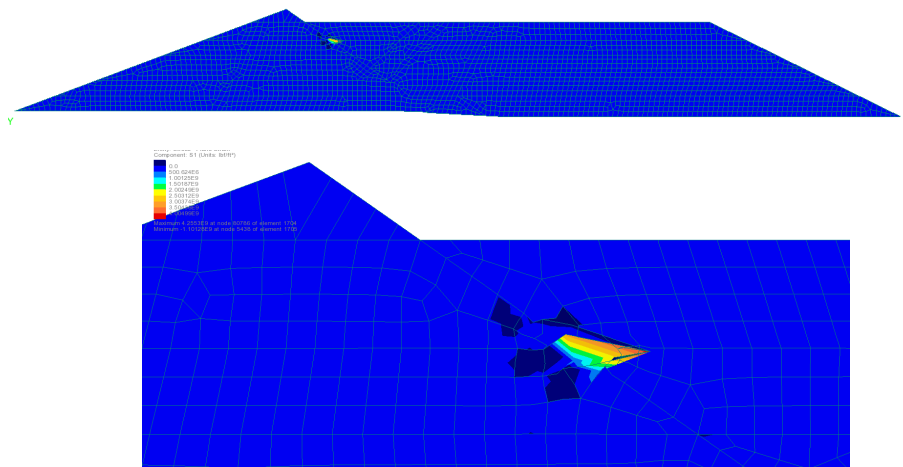


Figure 7: $\alpha=0.01$ - Displaced shape at failure

Finally, at value of $\alpha=0.1$ the solution runs to the end. In figure 7, the positive maximum principal stresses are shown. They occur mainly along the upstream edge of the main

dam and also along the coffer dam/main dam boundary. Also visible is the tensile stresses carried by the concrete block.

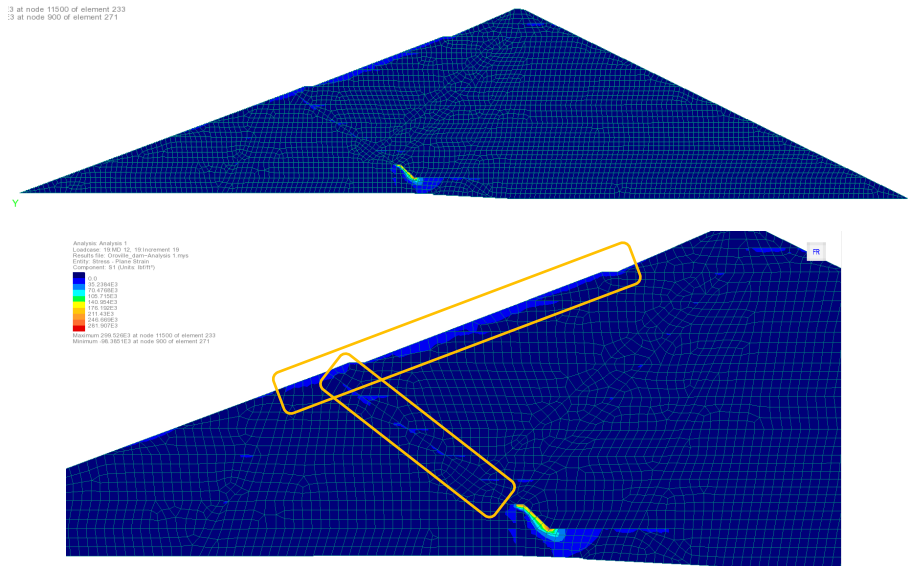


Figure 7: $\alpha=0.1$ – Contours of maximum principal stress at end of analysis

As mentioned, the stiffness of the soil depends on the confining stresses. To approximate these stresses the elements in a new layer are introduced with a nominal stiffness derived from the assigned K_0 value. The calculated stresses are then applied as initial stresses to the elements and the solution repeated. As the initial stresses are equal to the gravity load there is little or no displacement in the elements of the layer during its initialisation.

The option to fix the displacements of the deactivated elements is used so that the new element layers are in their correct position when activated.

Comparison

Results from two analyses are compared. In the first, the soil layer is activated in a single increment. In the second, the soil is activated over four increments with the gravity force applied equally in each. After applying the full gravity load, the displacements in the layer are reset.

Figure 8 shows the position of sensors placed in the main dam during its construction. The sensors U and I through to 7 measured horizontal displacements whilst the remaining sensors measured vertical displacement or settlement.

The zone marked in yellow indicates the location of the sensors whose data is shown in figure 9. The orange line and dots are the results for the single step analysis and the grey dots show results for the analysis in which the load was applied in four equal increments.

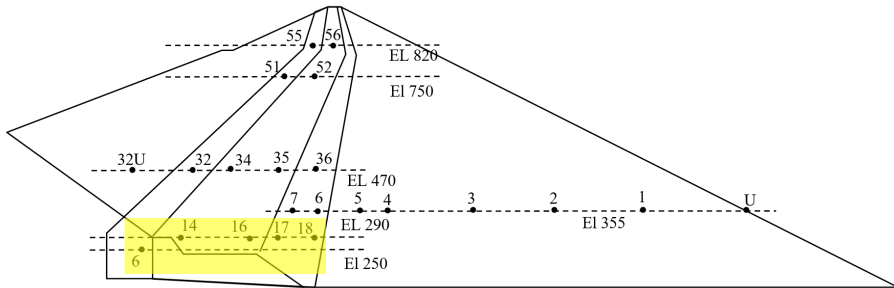


Figure 8: Location of displacement sensors in main dam

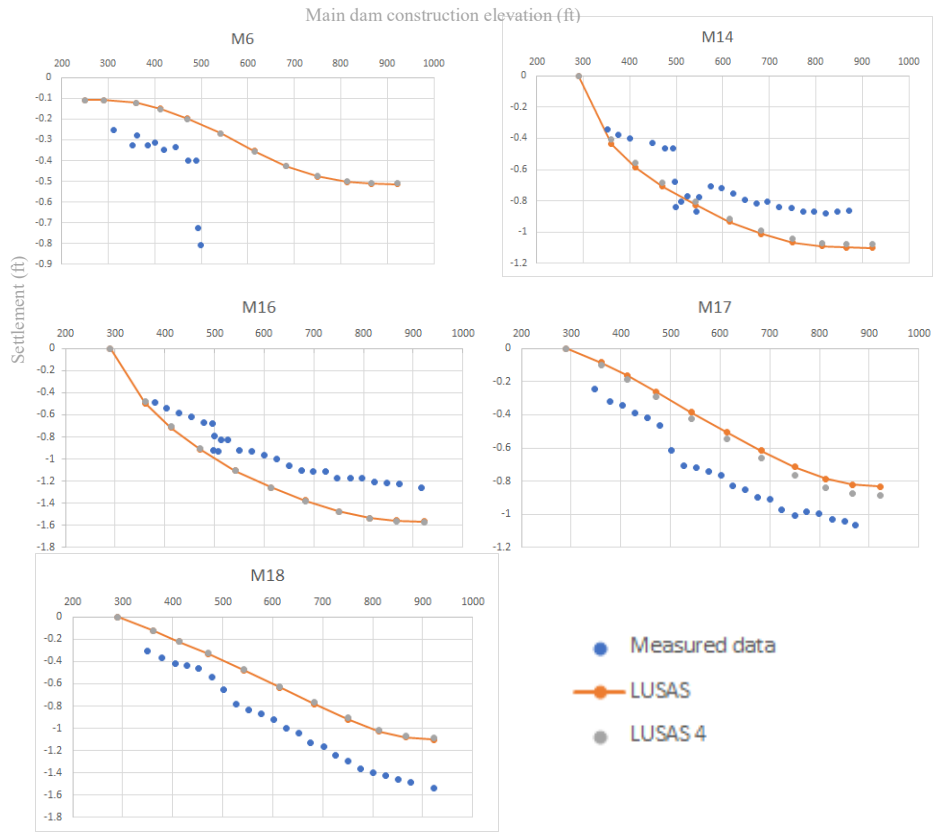


Figure 9: Settlements during construction at lower elevation

Figure 10 shows the location of the intermediate level sensors and figure 11 their measured data and solutions.

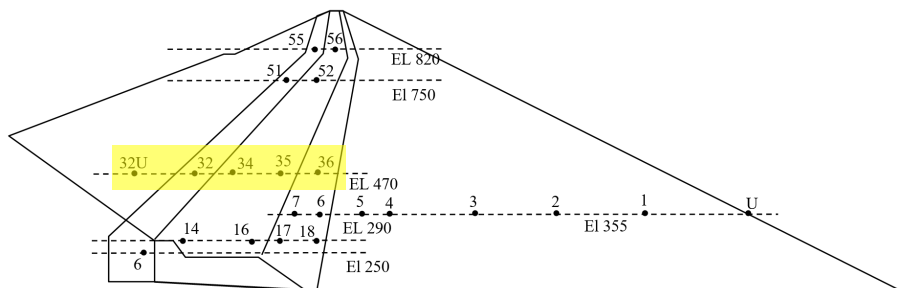


Figure 10: Location of intermediate level sensors in main dam

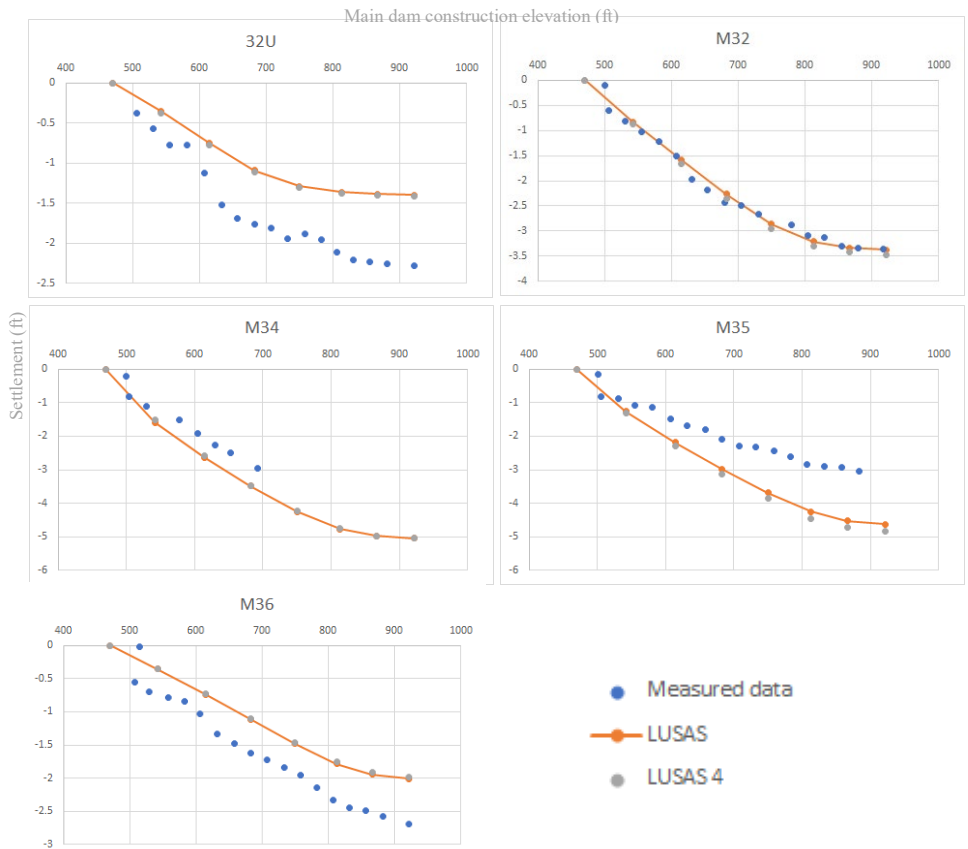


Figure 11: Settlements during construction at intermediate elevation

Figure 12 shows the location of the high level sensors and figure 13 their measured data and solutions.

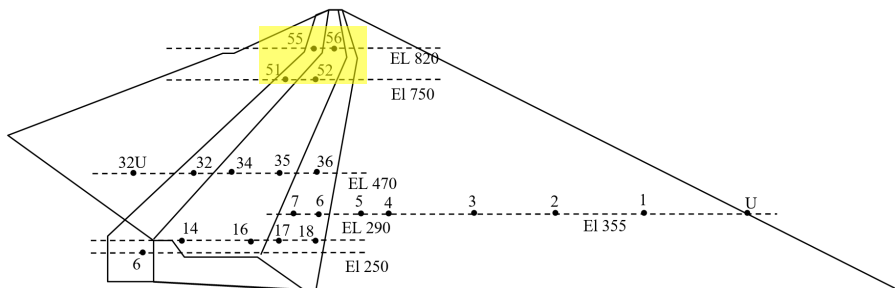


Figure 12: Location of high level sensors in main dam

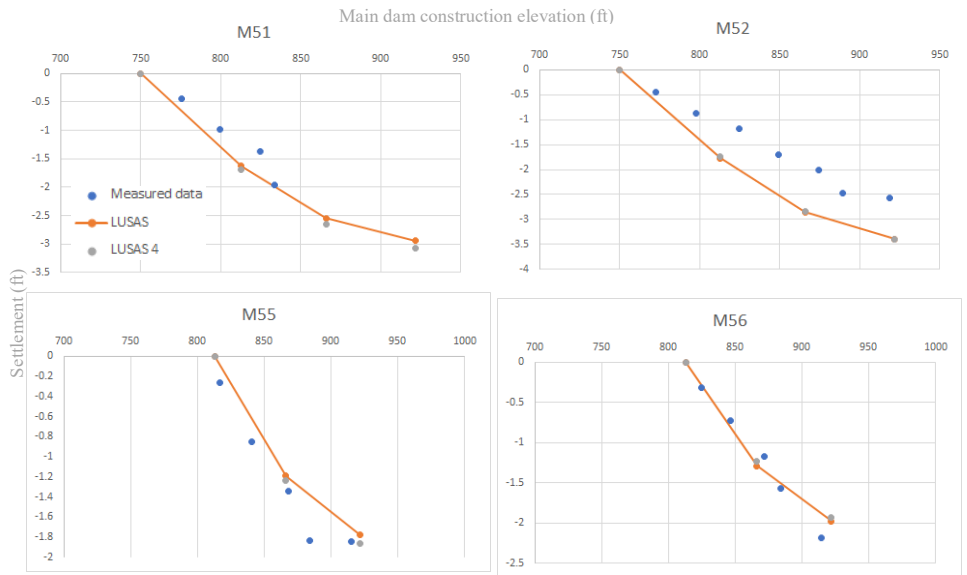


Figure 13: Settlements during construction at high elevation

Figure 14 shows the location of the sensors which measured horizontal displacement and figure 15 their measured data and solutions.

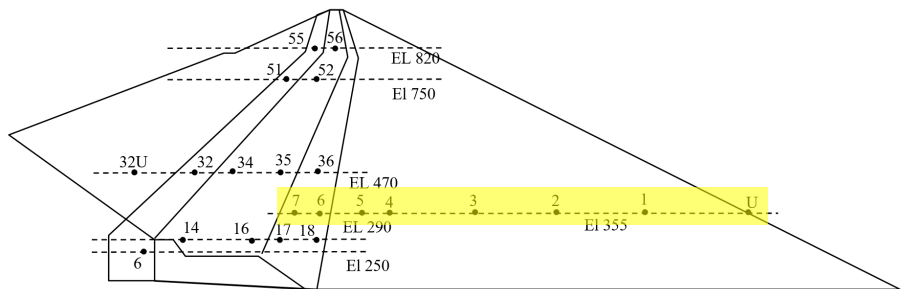


Figure 14: Location of horizontal displacement sensors

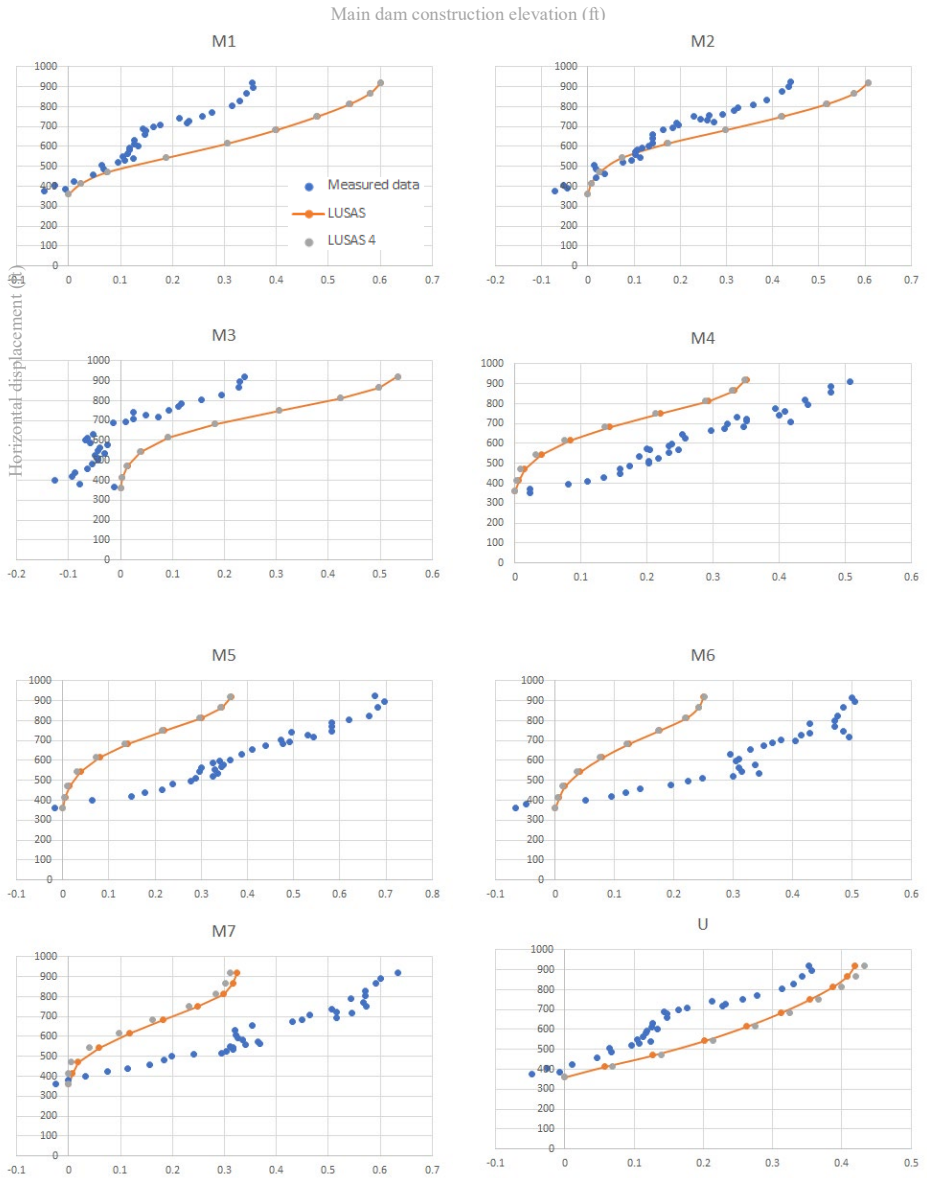


Figure 15: Horizontal displacements during construction

In general, there is good prediction of the settlements with the better predictions at the higher elevations. The horizontal displacements are also in reasonable agreement. The

use of four increments did not produce any significant changes to the results even though it is a better representation of the loading of the soil.

Finally, figure 16 shows contours of the final displacements and figure 17 the contours of vertical stress.

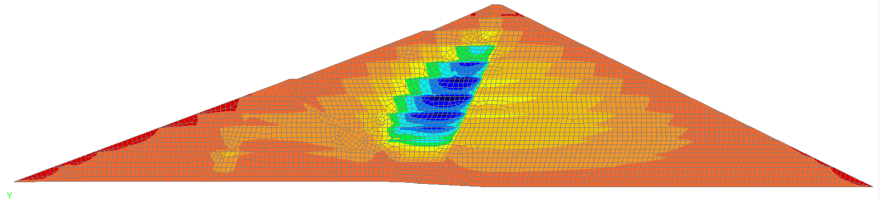


Figure 16: Contours of final displacements

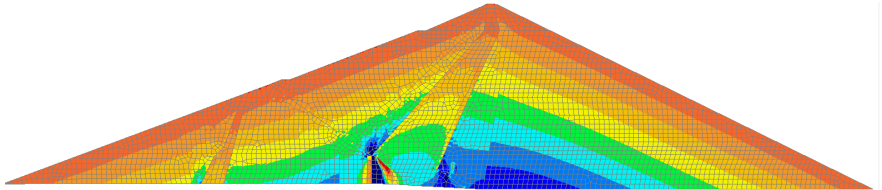


Figure 17: Contours of final vertical stresses

References

- [1] Kulhawy F.H. and Duncan J.M., Stresses and movements in the Oroville Dam, ASCE J.Soil Mech.Foundations Div., p653-665, 1972.

